This article has been accepted for publication in a future issue of this journal, but has not been fully edited. Content may change prior to final publication. Citation information: DOI 10.1109/TIA.2017.2756032, IEEE Transactions on Industry Applications

Dynamic Power Management and Control of PV PEM fuel Cell based Standalone AC/DC Microgrid Using Hybrid Energy Storage

Rishi Kant Sharma, *Student Member IEEE* and Sukumar Mishra, *Senior Member IEEE*

Abstract – **In this paper, dynamic power management scheme is proposed for standalone hybrid AC/DC microgrid which constitutes photovoltaic (PV) based renewable energy source, proton exchange membrane (PEM) fuel cell (FC) as a secondary power source and battery-supercapacitor as hybrid energy storage. The power management algorithm accounts for seamless operation of microgrid under various modes and state of charge (SoC) limit conditions of hybrid energy storage, when all the sources, storages and loads are connected directly at the dc link. The power management scheme (PMS) generates current references for dc converter current controllers of fuel cell, battery and supercapacitor. The average and fluctuating power components are separated using moving average filter. The dc link voltage regulation under dynamic changes in load and source power variation is proposed. Also, PV power curtailment through control is formulated. The proposed power management is modified and extended to multiple photovoltaic generation system and batteries with all the sources and storages geographically distributed operating under multi-time scale adaptive droop based control with supervisory control for mode transition. The proposed power management scheme is validated using simulation results. Also, FPGA/Labview based laboratory scale experimental results are presented to validate the power management scheme under various critical conditions.**

Index Terms—**PV, PEM fuel cell, power management, supercapacitor, voltage source converter, standalone AC/DC microgrid, Moving average filter, Multi-time scale, droop.**

I. INTRODUCTION

The demand of Hybrid AC/DC microgrid (MG) has increased significantly with increased penetration of renewable energy sources such as photovoltaic array (PV) at low voltage ac distribution sector. Increased number of dc loads such as plug-in vehicle, telecom load, central computer center, emphasizes the need of evolving microgrid suitable for both ac and dc loads [2]. The key challenges involves regulation of voltage and frequency of ac microgrid, dc link voltage regulation for both ac/dc system, unbalanced load operation as well as dynamic power balance due to- intermittency of renewable energy sources and uncertain nature of load variation [1]. The PEM fuel cell (FC) is an electrochemical device which provides a reliable steady state power however, is unable to meet the power transients owing to its slow response of internal thermodynamic and electrochemical process [3]-[6]. The system is often subjected to sudden change in load and source powers (PV) which leads to high fluctuation at dc link voltage and may affect the MG performance [1]. To avoid such contingencies, hybrid energy storage (HES) which is combination of high energy density and high power density needs to be introduced to supply/absorb steady state and transient power components in MG [8]-[9]. Thus, hybrid power source comprising PV as a primary source and fuel cell as a secondary source along with battery-supercapacitor (SC) as HES is a promising combination to operate the system in standalone mode [7].

The dynamics of variation in ac/dc load as well PV power are reflected at dc link voltage. Thus, its control plays determined role in dynamic power management of MG. In [6], fuzzy logic controller based on flatness property for dc voltage regulation is used for PV, FC and SC standalone system. The power reference of FC is obtained using low pass filter (LPF) and does not consider the over and under-utilization of H_2. The LPF introduces lag in the reference power generation of FC so SC has to supply both transient and constant power. Due to this SC voltage will hit its high/low limit frequently. In [7], with application of PV, FC, and battery-SC for DC system, has reduced the burden on SC by using battery-SC combination. The operation of PV at off maximum power point (MPPT) based on power management scheme is the key issue which should be considered carefully. In [10], operation of PV, FC and SC is presented for islanded microgrid under unbalanced and nonlinear load condition. The paper lacks the effective energy management.

The separation of average and transient power component for battery and SC is also a key issue. In [14], wind/load power fluctuations are mitigated using battery-SC combination where the average current reference is obtained by passing load current through low pass filter (LPF). Also, in [11], dc link voltage controller generates average component of current references through LPF. This LPF introduces significant time lag and dominant pole near to origin which may hamper system stability. In [12] and [13], moving average filter (MAF) computes time average value and provides

This work is partially supported by DST, Govt. of India under its project "UK India Clean Energy Research Institute" with project no. RP03413G and partially supported by Department of Electronics and Information Technology (DEITY), Govt. of India under Visvesvaraya PhD Scheme.
The authors are with Department of Electrical Engineering, Indian Institute of Technology, Delhi, 110016, India. (email-rishikant.iitd@gmail.com, sukumar@iitd.ac.in)

This article has been accepted for publication in a future issue of this journal, but has not been fully edited. Content may change prior to final publication. Citation information: DOI 10.1109/TIA.2017.2756032, IEEE Transactions on Industry Applications

average current reference without much lag and instability.

The multi-time scale control presented in [20]-[21], depends on hierarchical control solving economic dispatch problem with exchange of power from grid as well as SoC optimization. While the proposed work does not involves solving any economic dispatch problem, day ahead scheduling and power exchange from grid, nor it relies on dedicated central controller for its operation. For parallel operation and proper current sharing of multiple DC sources (DG) with converters in a distributed way, the output voltage reference of the converter operates in voltage droop mode defined by virtual resistance [17]. The multi-time scaling is categorized as (i) slow time scale DGs and (ii) fast time scale DGs. The conventional method to obtain muti-time scale droop for DGs with different dynamic responses utilizes the concept of virtual output impedances where the droop constant D_i is multiplied with low pass filter for slow time scale DGs and multiplied by high pass filter for fast time scale DGs [15], [16] and [22].

In this paper, two dynamic power management schemes are proposed for two different hybrid AC/DC microgrid configurations. The first configuration (MG1) consist of single PV and PEM fuel cell based hybrid power sources, single battery and supercapcitor based HES with dc loads and three phase inverter fed ac loads. Here, all the sources and HES are interfaced to dc link directly through their dc-dc converters, assuming they are at same geographical location, as presented in Fig. 1. The second configuration (MG2), consist of multiple PVs, single PEM FC, multiple batteries (BES) and single SC with dc and ac loads. Here, all the sources and storages are interfaced to dc link through cable connected at their individual dc-dc converters such that they are geographically distributed, as shown in Fig. 6.The proposed dynamic power management scheme (PMS) plays key role in dc link voltage regulation, current references generation and reference current tracking by current controller to drive dc-dc converters of PV, FC, SC and battery. The main contributions of the proposed dynamic power management scheme for MG1 and MG2 are

1. For MG1, current reference generation for PEM FC, Battery and SC using single dc link voltage controller.
2. For MG1, separation of average and transient current references using moving average filter (MAF).
3. For MG1, allocation of different current references to input current controllers of dc converters of PEM FC and HES by mode based power management algorithm to drive the system seamlessly from load dominating condition to generation dominating condition while maintaining power supply reliability even if the battery SoC and SC voltage are in limit condition.
4. The operation of PEM FC with effective utilization of H_2 is also ensured. Also, control based de-rating operation of PV boost converter is presented.
5. For MG2, muti-time scale adaptive droop based control with input current controller to operate the DGs in distributed way is proposed. A novel MAF based droop is used for time-scaling of fast and slow DGs. The SoC based adaptive droop is proposed for operation of multiple BES.
6. For MG2, supervisory control based mode transition signal employing low bandwidth communication (LBC) is proposed to operate the sources/storages in droop mode/ MPPT Mode/ SoC control mode/ Voltage control mode.

The Section II underlines the hybrid AC/DC microgrid configuration 1, Section III explains the proposed power management scheme for MG1, Section IV and V deals with hybrid AC/DC microgrid configuration 2 and its power management scheme followed by simulation/ experimental results in Section VI and Section VII concludes the work.

II. HYBRID AC/DC MICROGRID CONFIGURATION 1

The hybrid AC/DC microgrid (MG1) configuration 1 consists of PV with boost converter and PEM fuel cell (FC) with boost converter, both interfaced directly at dc link, as shown in Fig. 1. It is supported by hybrid energy storage (HES) comprising battery and supercapacitor (SC) interfaced directly to dc link through bidirectional DC-DC converters (BDC). The load consists of dc load and three phase ac load fed by three phase voltage source converter (VSC). Fuel cell generates only steady state power to meet the excess power demand in case of very less/no PV power is available. The HES supports both the steady state as well as transient power changes in generation and loads. It also assists the fuel cell to slowly ramp up its generation from minimum/zero value to the reference value. The SC supports transient/fluctuating as well as oscillatory power changes and is insufficient to supply/absorb constant power changes (for long time duration) due to its low energy density. While battery support constant power changes due to its high energy density, it may also supply transient power (only under crucial circumstances). The VSC operates in voltage control mode with fixed frequency obtained from voltage controlled oscillator [1]-[2]. It supplies three phase ac load or three single phase ac loads. The PV power curtailment is obtained by operating it on the linear characteristic of PV curve between MPP (V_{mp}) point and open circuit (V_{oc}). The modelling of PV connected to boost converter for MPP, Battery and SC connected to dc link through BDC and VSC control is discussed in detailed in [13].

Modelling and Control of PEM Fuel Cell

Some of the important relations that describes the modelling of PEM fuel cell are as follows [4]-[5]. Fuel cell stack current and hydrogen flow are related as

$$q_{h2}^{r} = N_0 I_{fc}/2F = 2K_r I_{fc} \tag{1}$$

Where , N_0 is the number of series fuel cells in the stack, I_{fc} is stack current (A), F is faraday's constant (C/Kmol) and K_r is modeling constant (Kmol/(sA)$^{-1}$).

This article has been accepted for publication in a future issue of this journal, but has not been fully edited. Content may change prior to final publication. Citation information: DOI 10.1109/TIA.2017.2756032, IEEE Transactions on Industry Applications

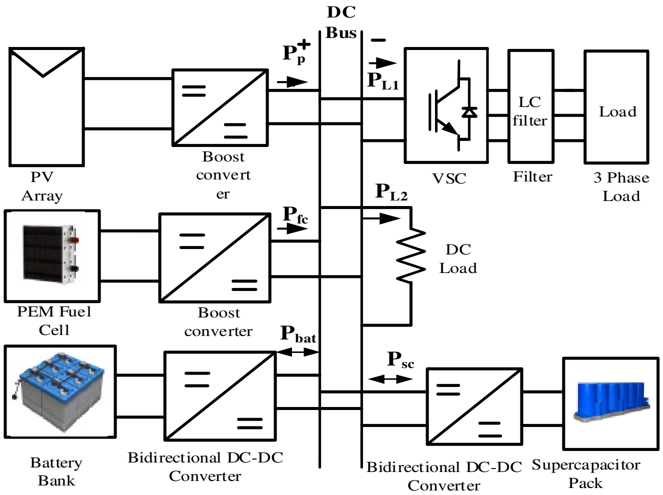

Fig. 1. Hybrid AC/DC Microgrid configuration 1

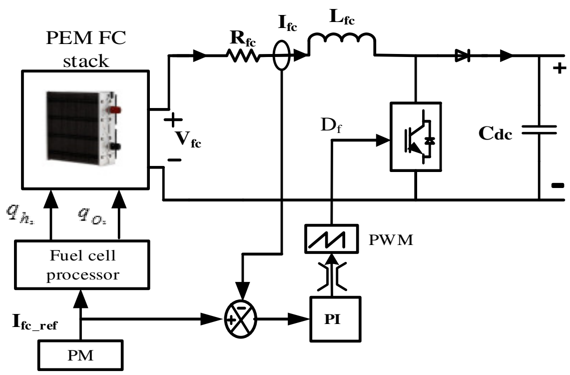

Fig. 2. PEM fuel cell with boost converter

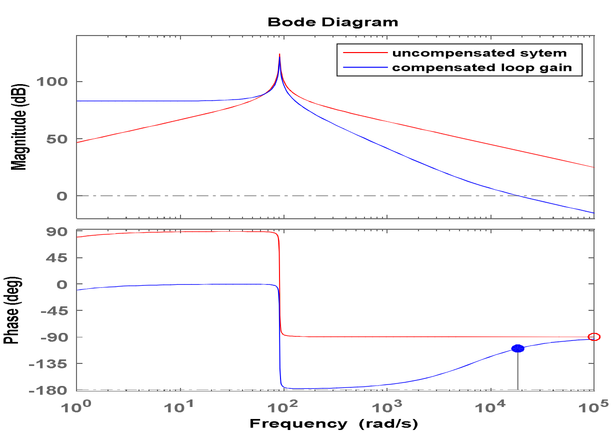

Fig. 3. Bode plot of compensated loop gain and uncompensated loop gain

The Polarization curve of the fuel cell gives the fuel cell voltage which is sum of the Nernst instantaneous voltage E, activation overvoltage η_{act} and ohmic overvoltage η_{ohmic} and is expressed mathematically as follows.

$$V_{cell} = E + \eta_{act} + \eta_{ohmic} \tag{2}$$

Where, η_{act} is function of oxygen concentration Co_2 and I_{fc}, η_{ohmic} is function of I_{fc} and and stack internal resistance R^{int} (Ω). Assuming constant O_2 concentration and constant temperature, (2) can be written as

$$V_{cell} = E - B\ln(C\,I_{fc}) - R^{int} I_{fc} \tag{3}$$

Where, B=0.04777 V and C=0.0136 A^{-1}. The Nernst voltage in terms of gas molarities is given by [4]

$$E = N_0\left[E_0 + \frac{RT}{2F}\log\left[\frac{\rho_{h2}\,\rho_{O2}^{0.5}}{\rho_{H20}}\right]\right] \tag{4}$$

Where, E_0 is open cell voltage (V). Hydrogen utilization factor (U) is defined as the ratio of H_2 reacted inside the stack to the injected H_2 into the tank and has value between 0 and 1.

$$U = q_{h2}^{r} \big/ q_{h2}^{in} \tag{5}$$

Values above 0.9 are indicative of over-utilization of hydrogen leading to fuel starvation and reduces its life and performance. On the other hand, values below 0.8 corresponds to under-utilization of hydrogen which indicates the presence of excess hydrogen, leading to sharp rise in output voltage and reduction in overall power efficiency. Thus, for optimal utilization of H_2 in fuel cell stack, stack current is limited by following criterion

$$\frac{0.8q_{h2}^{in}}{2K_r} \le I_{fc} \le \frac{0.9q_{h2}^{in}}{2K_r} \tag{6}$$

The current reference I_{fc_ref} obtained from the power management scheme generates the H_2 reference given by

$$q_{h2}^{ref} = \frac{2K_r I_{fc\_ref}}{U_{opt}} \tag{7}$$

In accordance to (6), the ramp rate of fuel cell reference current is controlled by current slope limiter (Ampere/sec) whose slope is based on current and power rating of PEM fuel cell [8]. Hence fuel cell avoids steep changes in load demands and guarantees matching the reactant delivery rate and the usage rate [9].

The PEM FC interfaced to dc link through boost converters operating in current mode control is shown in Fig.2. A conventional PI controller is implemented to track the reference current signal obtained from power management scheme and generates duty ratio to boost the fuel cell voltage to reference dc link voltage. The transfer function of fuel cell boost inductor current to converter duty ratio is given by [8],

$$\frac{\hat{\imath}_{FC}(s)}{\hat{d}_f(s)} = \frac{\frac{I_{FC}}{(1-D_f)}\left(1 + \frac{V_{dc}C_{dc}s}{(1-D_f)}\right)}{s^2 L_{FC}C_{dc} + sR_{FC}C_{dc} + (1-D_f)^2} \tag{8}$$

Where, L_{FC}, R_{FC}, and I_{FC} are the inductance, resistance and current of boost converter inductor respectively, D_F is converter duty ratio, V_{dc} and C_{dc} are dc link voltage and capacitance respectively. The transfer function (8) is compensated using proportional integral (PI) controller to obtain stable compensated system as well as ensure zero or very less steady state tracking error. The compensated loop gain is stable with phase margin of 70^0 and bandwidth around 2500 Hz, as shown in Fig.3.

III. PROPOSED POWER MANAGEMENT SCHEME 1

The proposed dynamic power management scheme (PMS) for MG1 is presented in Fig. 4. It comprises of current

This article has been accepted for publication in a future issue of this journal, but has not been fully edited. Content may change prior to final publication. Citation information: DOI 10.1109/TIA.2017.2756032, IEEE Transactions on Industry Applications

references generation, mode selection power management algorithm (PM), tracking of current references by current controllers and duty ratio generation for PWM switching pulses for different converters interfaced to sources and HES.

A. Reference Current Generation by PMS

The power balance in hybrid AC/DC microgrid is ensured by controlling power at the dc link. The total dc link power (average and transient) is the summation of power injected by the primary and secondary source, difference of power absorbed by ac and dc loads and sum/difference of power supplied/absorbed by the HES. The total power required to maintain the dc link is categorized as (i) average power component (p_{avg}) due to slow changes in PV/FC power and load power, (ii) oscillatory power component caused due to instantaneous ac power (p_o) of inverter fed load and (iii) transient power component (p_T) which arises due to sudden changes in PV power and ac/dc loads. Thus, the power balance equation of hybrid AC/DC Microgrid at dc link comprising above three component is given by (9)

$$\begin{aligned} p_{pv}(t) + p_{fc}(t) \pm p_{sc}(t) \pm p_B(t) - p_L(t) \\ = p_{dc}(t) = v_{dc} i_{dc} \\ = p_{avg}(t) + p_o(t) + p_T(t) \end{aligned} \tag{9}$$

Where, $p_{pv}(t)$,$p_{fc}(t)$, $p_{sc}(t)$ and $p_B(t)$ are the PV, FC, SC and battery power respectively, $p_L(t)$ is the sum of ac and dc load power, $p_{dc}(t)$ is the total dc link power, v_{dc} *and* i_{dc} are the dc link voltage and current respectively. An i_{dc} is the effective reference current for PMS so denoted by $i_{\_ref}$. It is the summation of the average current reference $i_{\_avg}$, oscillatory $i_{\_O}$ and transient current reference $i_{\_T}$.

$$i_{\_ref} = i_{\_avg} + i_{\_O} + i_{\_T} = \left(K_{pvdc} + \frac{K_{ivdc}}{s}\right)(v_{dcr} - v_{dc}) \tag{10}$$

Where, K_{pvdc} and K_{ivdc} are the proportional and integral gain of the outer dc link voltage controller, v_{dcr} is the reference value of dc link voltage. The average component of the reference current $i_{\_avg}$ is extracted by filtering $i_{\_ref}$ through moving average filter which computes the time average of the signal and does not introduces significant time delay unlike low pass filter [13]. The transient and oscillatory component of reference current is obtained by subtracting average current reference from total reference current, thus time scaled references are obtained.

$$i_{\_O} + i_{\_T} = i_{\_ref} - i_{\_avg} \tag{11}$$

Now, the fuel cell reference current is obtained by limiting the ramp rate of $i_{\_avg}$ through current slope limiter as discussed in Section II. Also, the obtained FC current reference must be within the maximum/rated value (Ifc_max) and minimum current limit (Ifc_min/zero) value based on rating of PEM fuel cell. Thus, Ifc_r1 is the fuel cell reference current obtained from PMS. The Ifc_r1 varies slowly and remains unaffected by transients caused by sudden variation in load and generation powers. Now, battery reference current is obtained to assist - the fuel cell under normal operating condition. The total average reference current is to be supplied by secondary source FC, however it is unable to meet the demand instantaneously. Thus, the difference of the average reference current and measured or reference fuel cell current is supplied to/by battery bank of HES. Hence, the battery reference current is given by

$$Ib\_r1 = I\_avg - Ifc\_r1 \tag{12}$$

Therefore, battery supplies/absorb average power and also assists PEM FC to meet the demand gradually under normal operation. The transient and oscillatory component of current reference (11) is added with proportional dc link voltage error (P) to improve dynamics of dc link voltage under transient [11]. This current serves as the supercapacitor reference current (Isc_r1).

$$Isc\_r1 = I\_ref - I\_avg + P(v_{dcr} - v_{dc}) \tag{13}$$

To maintain the state of charge (SoC) of battery when it reaches lower SoC limit condition (SoC_{BL}), the battery reference current is obtained from SoC control loop which is secondary control and operation is initiated by power management algorithm (PM). The error of reference SoC and estimated SoC is minimized using PI controller to generate battery reference current (Ib_r2) to charge the battery from the available power sources.

$$Ib\_r2 = \left(K_{ps} + \frac{K_{is}}{s}\right)(soc_{br} - soc_b) \tag{14}$$

Where, K_{ps} and K_{is} are the proportional and integral gain of SoC control loop of battery respectively, soc_{br} is the reference SoC value of battery to be maintained. Similarly, supercapacitor voltage control loop is considered to maintain the supercapacitor voltage when it reaches the minimum voltage limit (V_{SCL}). The SC voltage control loop uses PI controller to generate SC reference current Isc_r2 to charge the SC to reference voltage.

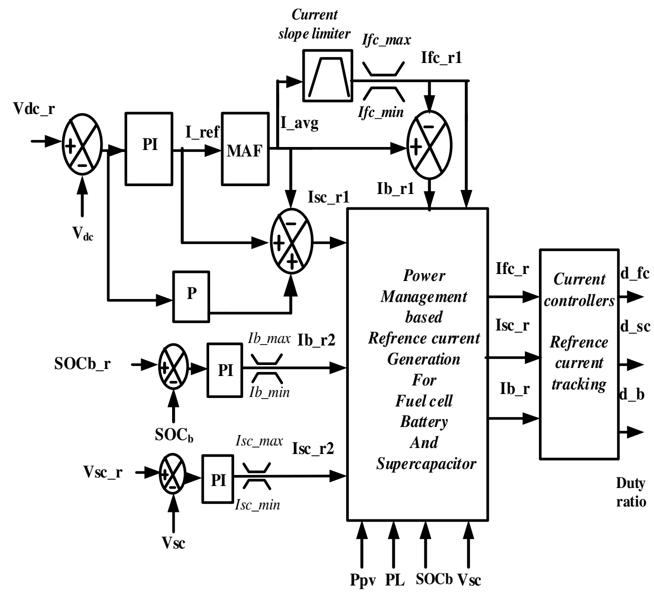

Fig. 4. Proposed power management scheme for hybrid AC/DC microgrid 1.

This article has been accepted for publication in a future issue of this journal, but has not been fully edited. Content may change prior to final publication. Citation information: DOI 10.1109/TIA.2017.2756032, IEEE Transactions on Industry Applications

$$Isc\_r2 = \left(K_{psc} + \frac{K_{isc}}{s}\right)(V_{SCr} - V_{SC}) \qquad (15)$$

Where, K_{psc} and K_{isc} are the proportional and integral gain of SC voltage control loop respectively, V_{SCr} is the reference SC voltage to be maintained.

B. Mode Based Power Management Algorithm (PM)

The power management algorithm (PM) drives the hybrid AC/DC microgrid seamlessly under different modes of operation. It considers following main criterion to operate the system normally. (i) difference of PV power and combine ac/dc load power (P_D) (ii) operation of battery under maximum (SoC_{BH}) and minimum (SoC_{BL}) SoC limits (iii) operation of SC under high (V_{SCH}) and low (V_{SCL}) voltage limit (iv) operation of fuel cell under maximum/rated current and minimum/zero current limit (v) operation of PV in MPPT mode or Off MPPT/de-rate.

$$P_D = P_{PV} - P_L \qquad (16)$$

Based on the value of difference in PV power (P_{PV}) and load power (P_L), three modes of operation are as follows:

(i) Mode I: Generation dominant mode ($P_D>0$)
(ii) Mode II: Load dominant mode ($P_D<0$)
(iii) Mode III: Normal mode ($P_D \cong 0$)

Mode I: Following conditions are formulated based on the SoC status of battery (SoC_B) and SC terminal voltage (V_{SC}).

Condition A: $SoC_{BL} < SoC_B < SoC_{BH}$ and $V_{SCL} < V_{SC} < V_{SCH}$

Since, PV power is more than the load requirement, the fuel cell will supply minimum/zero reference current to meet load demand while battery and supercapacitor will charge themselves as per the current references generated.

$$Ifc\_r = Ifc\_min, Ib\_r = Ib\_r1, Isc\_r = Isc\_r1 \qquad (17)$$

Condition B: $SoC_B > SoC_{BH}$ and $V_{SCL} < V_{SC} < V_{SCH}$

When battery hits high SoC limit and is unable to charge itself then its reference current is made zero. Now, SC control the dc link voltage and takes the total reference current i_{ref} to charge itself. Since, SC is not suitable for continuous charge/discharge hence PV power is curtailed therefore PV de-rating is carried out to make the reference SC current (Isc_r) zero. Consequently, MPPT mode is disabled and current duty ratio of PV boost converter (D_1) is held constant. Now, the de-rating controller gives reference duty ratio (D_2) which is subtracted from the current duty ratio, as shown in Fig. 5.

$$Ifc\_r = Ifc\_min, Ib\_r = 0, Isc\_r = I\_ref \qquad (18)$$

Condition C: $SoC_{BL} < SoC_B < SoC_{BH}$ and $V_{SC} > V_{SCH}$

When SC voltages becomes greater that its upper threshold V_{SCH}, then it is unable to absorb power, hence its current reference is reduced to zero. Now, battery controls the dc link voltage and total reference current is supplied by it.

$$Ifc\_r = Ifc\_min, Ib\_r = I\_ref, Isc\_r = 0 \qquad (19)$$

Condition D: $SoC_B > SoC_{BH}$ and $V_{SC} > V_{SCH}$

When battery SoC exceeds its upper threshold as well as SC voltages exceeds V_{SCH}, then HES is unable to absorb any power. Thus, the dc link voltage will start increasing and make the system unstable. To counter these effects, PV MPPT mode-

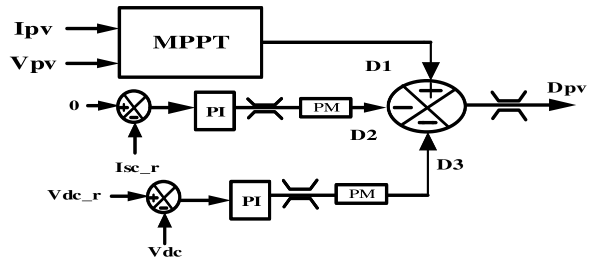

Fig. 5. PV power de-rating loop based on power management

- is disabled and current duty ratio is held constant. Now, dc link voltage control loop generates the corresponding duty ratio (D_3) which is subtracted from the current duty ratio, as shown in Fig. 5.

$$Ifc\_r = Ifc\_min, Ib\_r = 0, Isc\_r = 0 \qquad (20)$$

Condition E: $SoC_B < SoC_{BL}$ and $V_{SC} < V_{SCL}$

The excess power is used to charge the battery and supercapacitor to reference values based on (14) and (15). In case, the excess power is insufficient to charge the battery and SC to reference value, V_{dc} decreases. Consequently, FC supplies the required power.

$$Ifc\_r = Ifc\_r1, Ib\_r = Ib\_r1 + Ib\_r2, \quad Isc\_r = Isc\_r1 + Isc\_r2 \qquad (21)$$

Mode II: In this case, PV always operates at MPPT. Similar to MODE I, important conditions are formulated and are given as follows.

Condition F: $SoC_{BL} < SoC_B < SoC_{BH}$ and $V_{SCL} < V_{SC} < V_{SCH}$

Since, load power is greater than the PV power so secondary source FC supplies required steady state power assisted by battery while SC provides transient/oscillatory power in accordance to the reference current generation.

$$Ifc\_r = Ifc\_r1, Ib\_r = Ib\_r1, Isc\_r = Isc\_r1 \qquad (22)$$

Condition G: $SoC_B < SoC_{BL}$ and $V_{SCL} < V_{SC} < V_{SCH}$

In this case, battery is unable to assist fuel cell hence its reference current is zero while, the SC supplies its power demand as well as that of battery.

$$Ifc\_r = Ifc\_r1, Ib\_r = 0 \quad Isc\_r = Isc\_r1 + Ib\_r1 \qquad (23)$$

Condition H: $SoC_{BL} < SoC_B < SoC_{BH}$ and $V_{SC} < V_{SCL}$

In this condition, SC is unable to supply transient power so battery supplies its reference power along with that of SC while steady state power is met by FC.

$$Ifc\_r = Ifc\_r1, Ib\_r = Ib\_r1 + Isc\_r1, \quad Isc\_r = 0 \qquad (24)$$

Condition I: $SoC_B < SoC_{BL}$ and $V_{SC} < V_{SCL}$

In this condition, FC will supply the average power required to meet load demand. However, without any of the storage element, it is unable to supply the power instantaneously hence if dc link voltage decreases and reaches near permissible limit then load shedding is initiated and microgrid is forced to operate under Mode III.

$$Ifc\_r = Ifc\_r1 or\ 0, \ Ib\_r = 0, \quad Isc\_r = 0 \qquad (25)$$

Mode III: In this mode, PV and load power are approximately same so PV operates at MPPT while supercapacitor controls

This article has been accepted for publication in a future issue of this journal, but has not been fully edited. Content may change prior to final publication. Citation information: DOI 10.1109/TIA.2017.2756032, IEEE Transactions on Industry Applications

the dc link voltage to supply/absorb the small oscillatory power.

$$Ifc\_r = Ifc\_min,\ Ib\_r = 0,\ Isc\_r = I\_ref \qquad (26)$$

IV. HYBRID AC/DC MICROGRID CONFIGURATION 2

The hybrid AC/DC microgrid configuration 2 (MG2) consists of multiple PV sources with their individual boost converters, multiple battery bank with their individual bidirectional converters, a supercapacitor pack with its bidirectional converter and a PEM fuel cell with its boost converters, connected to same dc link through cable having impedance mainly resistive at steady state. The dc loads and three phase inverter fed ac load are also connected at dc link, as presented in Fig. 6. Since, the sources and storages are geographically distributed hence, needs a modified power management scheme for reliable operation.

V. PROPOSED MULTI-TIME SCALE DROOP BASED POWER MANAGEMENT SCHEME

The power management scheme for MG 2 is modified and extension of that proposed in Section III. In this scheme, the current reference generation and its tracking are executed locally in a distributed way based on individual system available measurements while mode transition signal is obtained from supervisory control using low bandwidth communication channel (LBC)[19], having access to system critical parameters responsible for mode change. To operate the microgrid (MG2) having sources with different dynamic response such as PEM FC, batteries and supercapacitor, a muti-time scale adaptive droop constituting MAF is implemented for proper power sharing and generation of current references while inner current controller tracks these references to drives the dc-dc converters by generating desired duty ratio.

A. Reference Current Generation and Tracking

The parallel operation and proper current sharing of multiple DGs with converters in a distributed way, the output voltage reference of the converter operates in voltage droop mode. Also, multiplication of measured voltage deviation with reciprocal of virtual resistance is done for proper current sharing [15].

$$V_{oi}^{*} = V_{dcr} - R_{di} * i_{oi} \qquad (27)$$

Where V_{oi}^{*} is output voltage reference, V_{dcr} is dc link nominal voltage, R_{di} is the virtual resistance or droop and i_{oi} is the output current of ith converter. The droop constant is defined as the reciprocal of virtual resistance and is given by

$$D_i = \frac{1}{R_{di}} = \frac{I_{ri}}{\delta(1-\delta)V_{ri}} \qquad (28)$$

Where I_{ri} and V_{ri} are rated output current and voltage of ith DG while δ is output voltage tolerance in percentage.

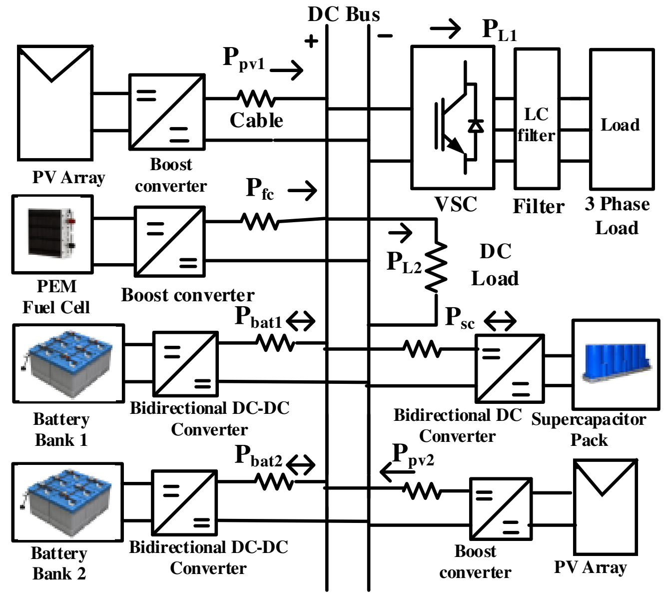

Fig. 6. Hybrid AC/DC Microgrid configuration 2

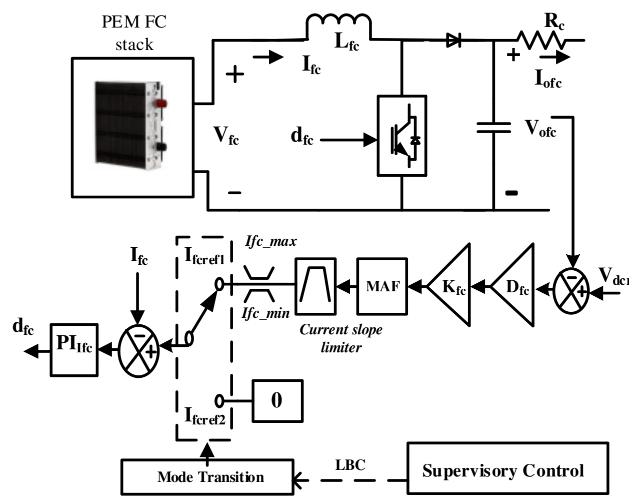

Fig. 7. PEM FC time scale droop based control.

The reference current for PEM fuel cell must be slow time scaled while satisfying criterion (6). The FC boost output voltage deviation is multiplied by droop constant D_{fc} to get desired output current sharing which is scaled by factor K_{fc} to obtain the corresponding input current. Now, the obtained input current reference is slow time scaled by passing it through MAF and current slope limiter to get the desired FC boost input current reference I_{fcref1}. The PI based input current controller tracks the desired current reference and generates the FC boost converter duty ratio d_{fc}, as shown in Fig. 7.

The reference dc link voltage of the DGs also considers the voltage drop due to cable resistance and is given by [18]

$$V_{dcr} = V_{dcn} + R_c * I_{oi} \qquad (29)$$

Where, V_{dcn} is the nominal dc link voltage, R_c is cable resistance and I_{oi} is the output current of ith DG. And, the scale factor K_i is given by

$$K_i = V_{oi}/V_{ini} \qquad (30)$$

Where, V_{oi} and V_{ini} are the output and input terminal voltage of the i[th] DG.

The supercapacitor converter output voltage deviation is multiplied by droop constant D_{SC} and scaled by factor K_{SC}. Now, the obtained current reference I_{SC1} is passed through MAF and its error with I_{SC1} serves as the SC converter input current reference I_{SCref1}. The I_{SCref1} is fast time scaled and shares the transient current using droop control. The obtained input current reference is tracked by PI controller to generate SC converter duty ratio d_{droop}, as shown in Fig. 8. The SC voltage control loop similar to (15) generates I_{SCref2} and inner PI current controller generates duty ratio d_{vsc} for SC converter.

The battery current reference must be slow time scaled as well as the current sharing must depend on its present SoC status, hence time scaled adaptive SoC based droop control is proposed. The adaptive SoC droop constant exhibits (i) the battery with higher SoC must be discharged at higher rate while battery with low SoC must be discharged at slow rate. (ii) The charge/discharge current shared must be proportional to their capacity (Ah). (iii) The battery with lower SoC must be charged at higher rate [18]-[19]. The proposed adaptive SoC based droop constant senses the output voltage deviation of the converter e_{bi}, and changes the droop constant value accordingly for the charge and discharge mode.

$$D_{bi,charge} = \frac{C_{bi}}{C_{bm}} \xi exp\big(\phi * (SoC_{BL} - SoC_i)\big),\ e_{bi} < 0$$
$$D_{bi,discharge} = \frac{C_{bi}}{C_{bm}} \xi exp\big(\phi * (SoC_i - SoC_{BH})\big), e_{bi} > 0 \tag{31}$$

Where, C_{bi} is the capacity of i[th] battery, C_{bm} is the capacity of battery with highest Ahr. ξ and ϕ are the tuning parameter. SoC_i is the SoC of the i[th] battery energy storage (BES). The obtained output current by multiplying droop constant with e_{bi} is now scaled by factor K_{bi} to get input current reference I_{bref2}. This current reference is slow time scaled by passing through MAF to get the desired BES converter input current reference I_{bref1}. The inner PI based current controller tracks the desired current reference and generates the converter duty ratio d_{droop}. The SoC control loop for BES similar to (14) generates current reference I_{bref3} and the inner controller tracks the reference current and generates duty ratio d_{SoC}, as shown in Fig. 9.

When multiple photovoltaic generation system geographically distributed are connected to dc link through cable, then they may operate either in MPPT mode or droop mode/OFF MPPT. The MPPT algorithm generates the reference PV voltage V_{pv}. The outer PI based voltage controller tracks the reference voltage and generates the inner current reference for boost converter I_{pvref2}. The PI based inner current controller tracks I_{pvref2} and produces duty ratio d_{mmpt} for boost converter [18]. For operation of PV at OFF MPPT, droop based control is adopted [19]. The output terminal dc voltage obtained using droop (27) and the error is passed to PI based voltage control loop which generates the boost converter input current reference I_{pvref1}. The PI based current controller tracks- I_{pvref1} and generates duty ratio d_{droop}, as shown in Fig. 10.

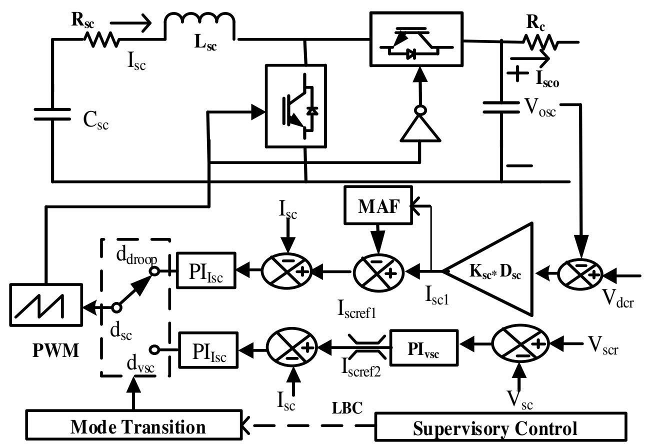

Fig. 8. SC time scale droop based control.

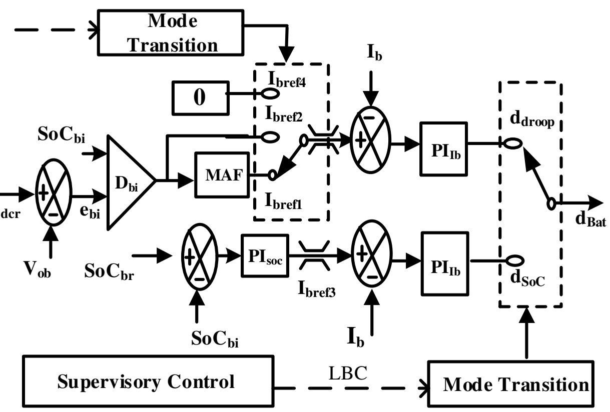

Fig. 9. BES time scaled adaptive SoC based droop control.

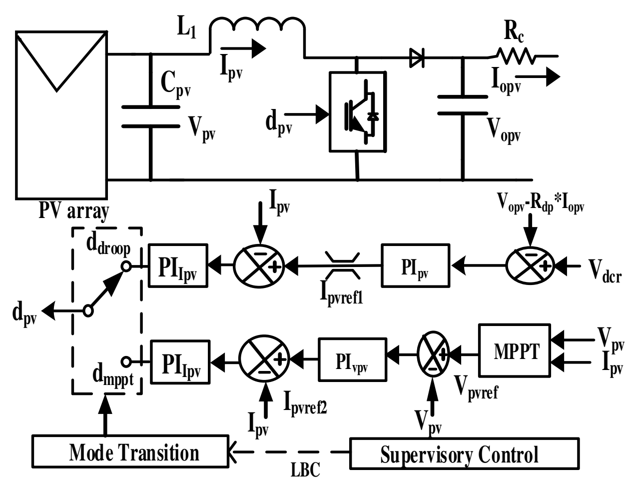

Fig. 10. PV MPPT/droop control.

B. Supervisory Control based Mode transition Algorithm

The proposed multi-time scale adaptive droop based PMS consists of parallel operation of DGs in a distributed way while supervisory control generates mode transition signal to drive system from load dominating to generation dominating mode using LBC. The supervisory control has access to critical

This article has been accepted for publication in a future issue of this journal, but has not been fully edited. Content may change prior to final publication. Citation information: DOI 10.1109/TIA.2017.2756032, IEEE Transactions on Industry Applications

parameters of system such as SoC_i, SoC_{BL}, SoC_{BH} ,V_{SC}, V_{SCL}, V_{SCH}, V_{dc}, V_{dcr} and $\Delta V_{dc} = V_{dcr} - V_{dc}$.

Mode I: *Generation dominating mode*: $\Delta V_{dc} > 0$.

Condition A: SoC_{BLi}< SoC_{Bi} < SoC_{BHi} and V_{SCL} < V_{SC} < V_{SCH}. All the PVs operate at MPPT and supply power based on d_{mmpt}. The SC absorbs transient power based on I_{SCref1} and operates in droop mode d_{droop}. The BESs shares the power based on adaptive droop $D_{bi,charge}$, with current I_{bref1} and duty ratio d_{droop}. The PEM FC does not supplies any power, $I_{fcref2} = 0$.

Condition B: SoC_{BLi}< SoC_{Bi} < SoC_{BHi} and V_{SC} > V_{SCH}.
The SC is unable to absorb transient power hence $I_{Scref3} = 0$, while BES shares both average as well as transient power therefore, mode transient signal switches to I_{bref2}. The PV operates at MPPT while FC supplies zero current (I_{fcref2}).

Condition C: SoC_{Bi} > SoC_{BHi} and V_{SC} < V_{SCH}.
When any one of battery hits SoC_{BH} and is unable to absorb any power, its reference current is reduced to zero, $I_{bref3} = 0$, while other BES will supply I_{bref1}. The SC supplies I_{scref1}, FC supplies I_{fcref2} while PV remains at MPPT mode.

Condition D: SoC_{Bi} > SoC_{BHi} and V_{SC} < V_{SCH}.
When both BES hits SoC_{BH}, then both the current reference are $I_{bref3} = 0$. The SC supplies I_{scref1} while FC supplies I_{fcref2}. Now, mode transition signal switches PV from MPPT mode to droop mode with I_{pvref1} and boost duty ratio d_{droop}.

Condition E: SoC_{Bi} > SoC_{BHi} and V_{SC} > V_{SCH}.
In this case BES as well as SC are unable to absorb any excess power, hence both of them supplies zero reference current and PV operates in droop mode to de-rate its power in accordance to load power and maintain dc link voltage under permissible tolerance. Therefore, $I_{bref3} = I_{Scref3} = I_{fcref2} = 0$.

Mode II: *Load dominating mode*: $\Delta V_{dc} < 0$.
In this case, All the PVs always operates in MPPT mode.

Condition F: SoC_{BLi}< SoC_{Bi} < SoC_{BHi} and V_{SCL} < V_{SC} < V_{SCH}
In this case, BES shares the average power and discharges based on adaptive droop constant $D_{bi,discharge}$, with I_{bref1} current reference and duty ratio d_{droop}. The SC supplies transient current I_{scref1} while PEM FC shares power in droop mode with current reference I_{fcref1}.

Condition G: SoC_{Bi} < SoC_{BLi} and V_{SCL} < V_{SC} < V_{SCH}
In this case, BES which hits its low limit operates in SoC control mode with current I_{bref4} and duty ratio d_{SoC}, while other BES discharge in adaptive droop mode. The SC supplies I_{scref1} in droop mode while FC supplies I_{fcref1} in droop mode.

Condition H: SoC_{BLi}< SoC_{Bi} < SoC_{BHi} and V_{SC} < V_{SCL}
In this case, SC is unable to supply transient power and mode transition signal switches to voltage control mode with I_{scref2} and d_{Vsc}. The FC supplies I_{fcref1} in droop mode.

Condition I: SoC_{Bi} < SoC_{BLi} and V_{SC} < V_{SCL}
The BES charges though SoC control loop while SC operates in voltage control mode, hence I_{bref4} and I_{scref2} while FC suppliesI_{fcref1}. This condition is common for both the modes.

VI. RESULTS AND DISCUSSION

A. Simulation Results 1

The hybrid AC/DC microgrid configuration 1 is simulated under various modes and conditions discussed above to validate the proposed dynamic power management scheme 1 under dynamic load and source power variation. All the components are modelled in Matlab/Simulink in simpowersystem domain and parameters used for simulation are presented in Appendix.

1). Scenario I:

During *t*=0 to *t*=4 s, the system is working in Mode II, Condition F as the PV power is less than load power, as shown in Fig. 12. The deficit power is supplied by fuel cell, battery and SC, according to (22). At *t*= 2 s, PV power changes from 6.4 kW to 7.4 kW while at *t*= 4 s, load power decreases from 7.6 kW to 5.5 kW. Now, the hybrid microgrid operates in Mode I Condition A. Consequently, FC power start decreasing while SC and battery absorb power to maintain dc link voltage, as illustrated in Fig. 13 and Fig. 15. The battery absorbs the average power while SC compensates the oscillatory and transient power as per (17), as shown in Fig. 15. At *t*=7 s, battery SoC reaches its maximum value SoC_{BH} (80%), hence system experiences critical Condition B and is presented in Fig.16. As a result, the power management scheme generates current references based on (18) and executes PV de-rating loop to match load and PV power, as shown in Fig. 12. At *t*=8 s, the load power decreases to 4.6 kW. Again, PV de-rating loop decreases the PV boost converter duty ratio to force the SC current zero, as shown in Fig. 12 and Fig. 14. At this instant, SC supplies/absorbs a very small oscillatory power. At *t* =11.45 s, SC voltage reaches its maximum value V_{SCH}, hence system enters into Mode I Condition D, as shown in Fig 16. Now, the dc link voltage is controlled to de-rate the PV power such that it power matches the load power, as presented in Fig. 12. At this instant, SC, battery and FC supply zero powers based on (20). Three phase line to line voltage of VSC output (380 V rms) and load current is shown in Fig. 17.

2). Scenario II:

In this scenario, load dominating mode conditions are simulated. At *t*=2 s, PV power reduces from 5.5 kW to 4.5 kW and at *t*=4 s, again reduces to 3.4 kW, as shown in Fig. 18 and Fig. 19. During *t*=0 to *t*= 6 s, load power of 6.4 kW is more than PV power hence the system operates in Condition F. The average deficit power is supplied by the FC assisted by battery and transient/oscillatory power being supplied by SC as per (22) and is shown in Fig. 19. At *t*=6.1 s, battery reaches its lower SoC limit SoC_{BL} (20%), as presented in Fig. 21. Now, the power management algorithm produces current references according to (23) as system experiences Condition G. At *t*=9.94 s, the SC voltage reaches its lower voltage limit V_{SCL}, therefore system experiences Condition I. Thus, PM produces zero current references for battery and SC while average current reference is supplied by FC as per (25) and the converter current controller track these references effectively,-

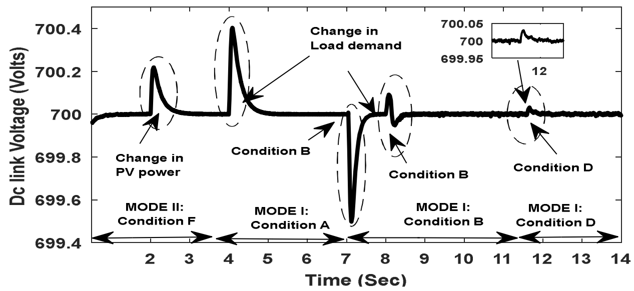

Fig. 11. Variation of dc link voltage scenario I

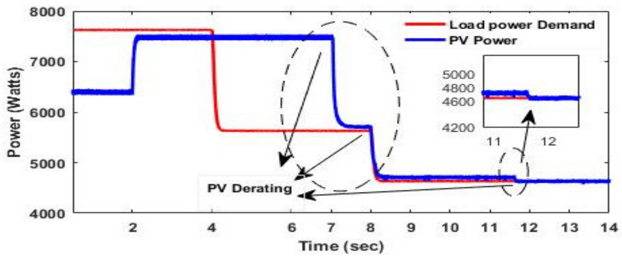

Fig. 12. Variation of PV power and load power

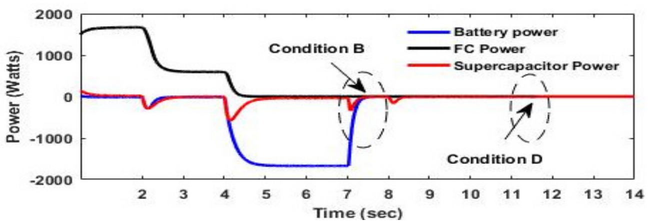

Fig. 13. Variation of Battery, SC and FC powers scenario I

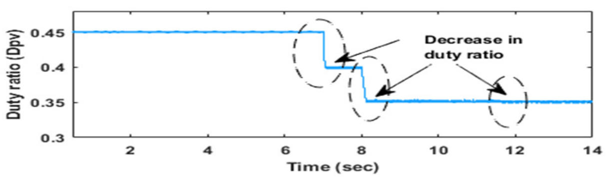

Fig. 14. Variation of PV boost converter duty ratio scenario I

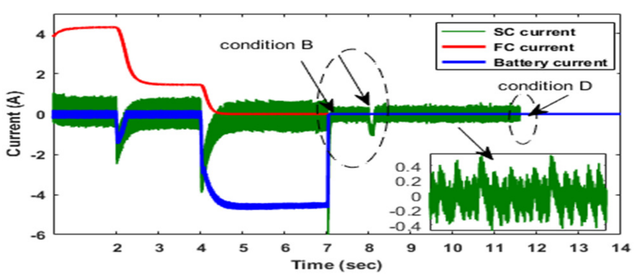

Fig. 15. Variation of SC, FC and battery currents scenario I

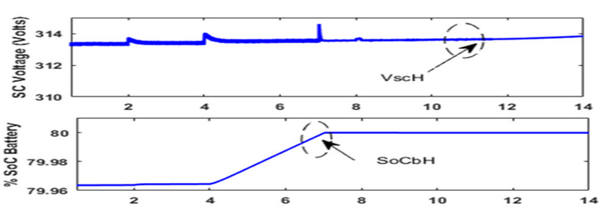

Fig. 16. Variation of SC voltage and % SoC of Battery scenario I

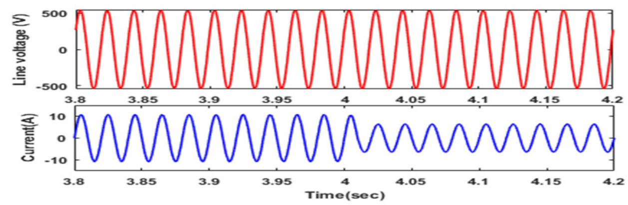

Fig. 17. Load voltage (L-L) and load current scenario I

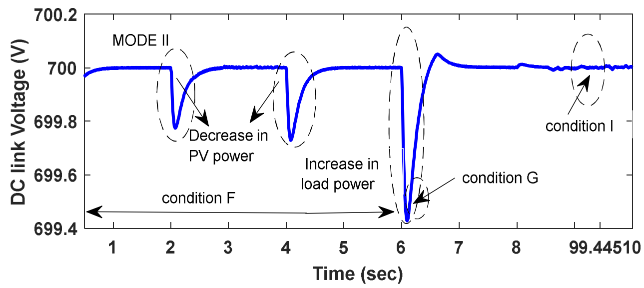

Fig. 18. DC link voltage variation scenario II

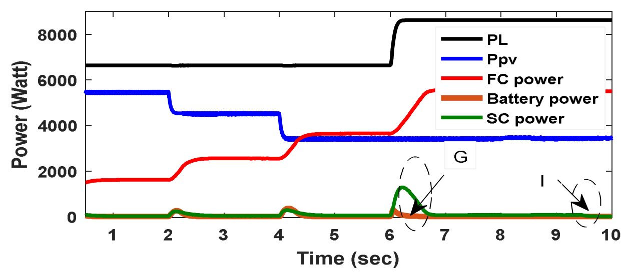

Fig. 19. PV, SC, FC, battery and load power scenario II

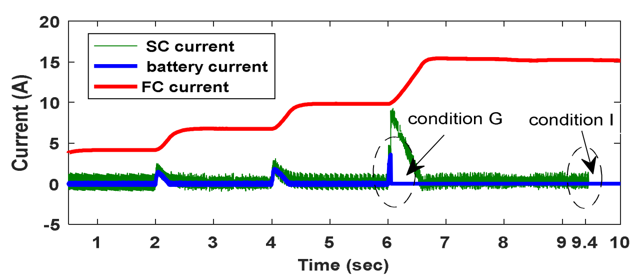

Fig. 20. Variations in SC, FC and battery currents scenario II.

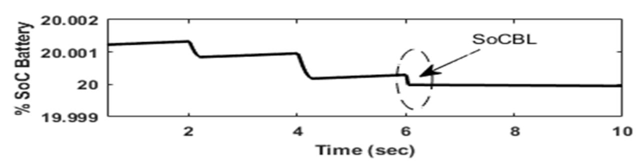

Fig. 21. Variations in % SoC of battery scenario II.

-as presented in Fig. 19 and Fig. 20. The dc link voltage and input current controllers maintains the dc link almost constant at 700V reference even when subjected to step change in load and source powers, as shown in Fig. 11 and Fig. 13.

B. *Simulation Results 2*

The PMS proposed in Section V is validated for MG 2, -

This article has been accepted for publication in a future issue of this journal, but has not been fully edited. Content may change prior to final publication. Citation information: DOI 10.1109/TIA.2017.2756032, IEEE Transactions on Industry Applications

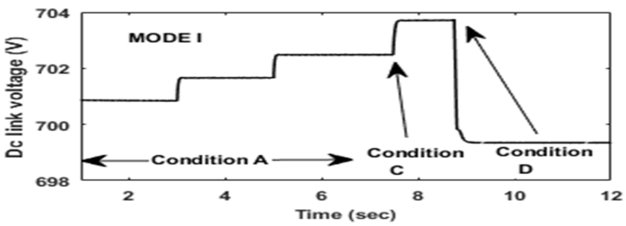

Fig. 22. DC link voltage variation

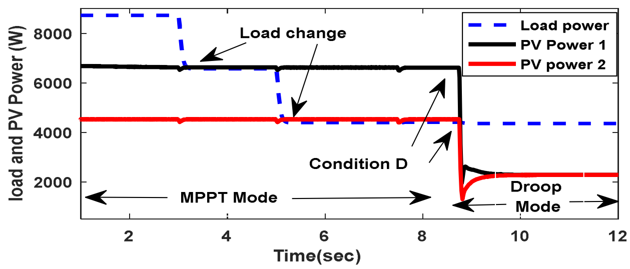

Fig. 23. PV1, PV2 and load powers.

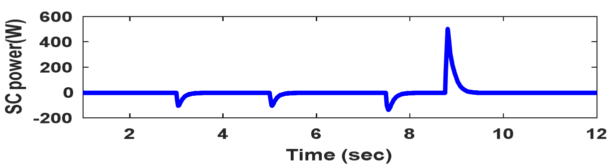

Fig. 24. Variations in SC power.

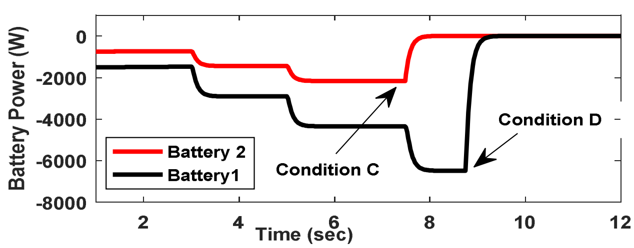

Fig. 25. Variations in BES powers.

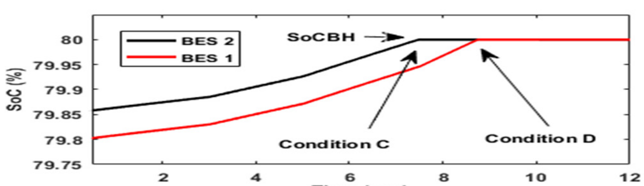

Fig. 26. Variations in % SoC BES

- presented in Fig.6. Initially MG2 is operating in generation dominating MODE I, Condition A. The load power changes from 8.73 kW to 6.57 kW at t=3 s and again decreases to 4.35 kW at t=5 s. The power supplied by PV1 and PV2 are 6.62 kW and 4.52 kW respectively, presented in Fig. 23. The BES1 of 20 Ahr with 79.8% SoC and BES 2 of 10 Ahr with 79.85% SoC, absorbs power based on adaptive droop (31). The power absorbed by BES 2 changes from 0.74 kW to 1.45 kW at t=3 s, and to 2.17 kW at t=5s, and hits its SoC_{BH} at 7.5 s, thus MG2 enters in Condition C. The BES 1 absorbed power changes -

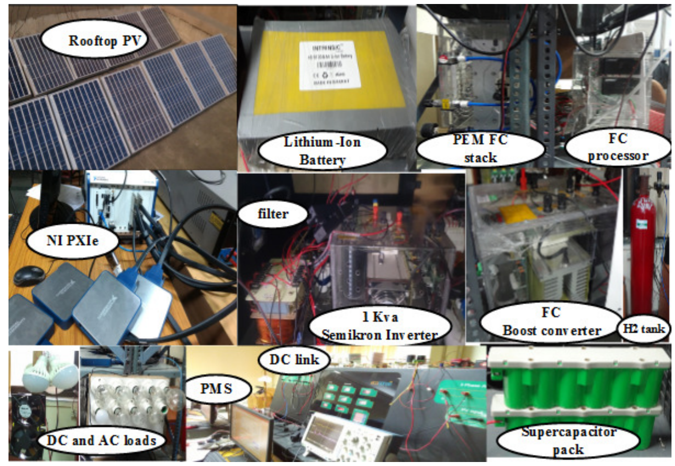

Fig. 27. Experimental setup

- from 1.5 kW to 2.9 kW at t=3 s, to 4.35 kW at 5 s and 6.5 kW at 7.5 s and hits it's SoC_{BH} at 8.75 s, shown in Fig. 25 and Fig. 26. Hence, the MG2 enters in Condition D, so the PVs changes its operation from MPPT mode to droop mode and shares same power of 2.27 kW, presented in Fig. 23. The SC supplies transient power while BES shares average power based on multi-time scale droop. The PEM FC supplies zero power. The dc link voltage rises from 700 V to 703.5 V till 7.5 s while decreases to 699.3 V at 8.75 s, as shown in Fig. 22. Thus, the presented PMS for MG2 is robust to mode transitions without any oscillations due to use of MAF based multi-time scale adaptive droop constant as compared to LPF based droop constant [15]-[16].

C. *Experimental Results*

The real time operation of the proposed MG1 with HES is implemented in FPGA platform which consist of Xilinx board programmed through National Instrument-PXIe chassis and analog signal acquisition by NI-PXIe 7853 R series channels. The proposed PMS is implemented in GUI based LABVIEW which provides switching pulses to all the converters and VSC. The hardware setup is presented in Fig. 27, consists of rooftop PV panels, 48 V lithium- ion battery, 32 V supercapacitor pack, H-1000 Horizon PEM FC stack with its processor and dry H_2 cylinder as well as boost and bidirectional converters. It also consists of 1 KVA Semikron inverter with LC filter. Ac bulb and dc Fan and light loads with controllable switch are used. The parameters for the experimental setup are given in Appendix. *Case (1)* corresponds to Condition F of Mode II. Here, PV power is assumed zero (night) and the total ac and dc load is met by FC and HES. At instant t_1, loads are switched ON. Initially, FC current is 0.2 A. At t_1, the battery supplies 0.25 A while SC supplies 0.4 A instantaneously. The FC current ramp up to 0.6 A in 4 s while, battery current goes to zero in same time duration. The SC current reduces to 0.2 A to supply oscillatory power component in the MG, as shown in Fig. 28. Note, that the negative current direction of battery and SC shows discharging. Again at t_2, the loads are switched ON.

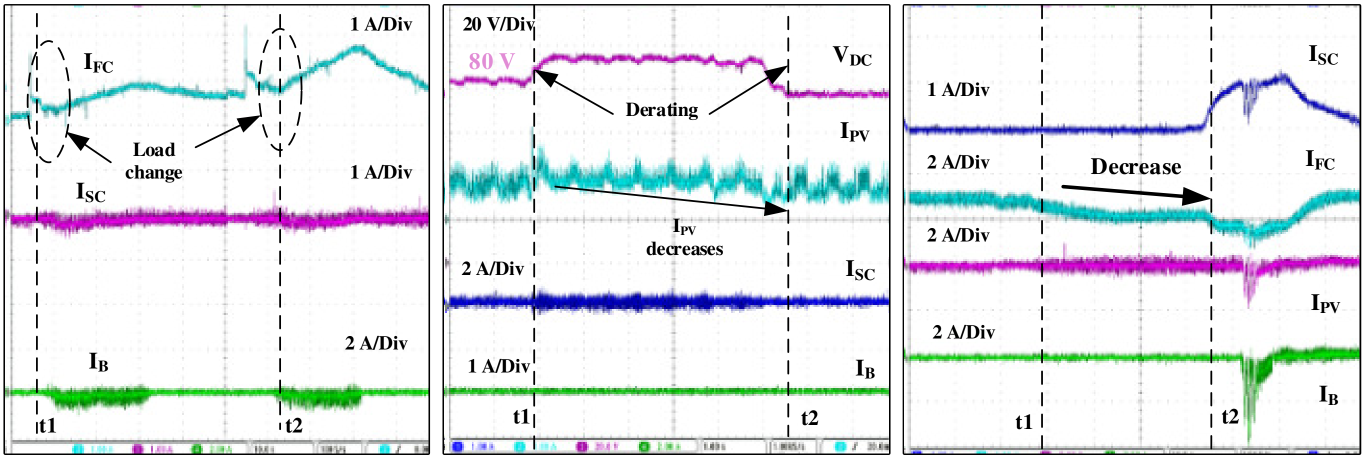

Case (1) Case (2) Case (3)

Fig. 28. Experimental results under various conditions.

The FC current ramps up from 0.6A and reaches 1 A in next 4s. The SC supplies transient 0.3A and then reduces to 0.2A. During this period, battery current increases from zero to 0.2A and then reduces to zero as FC reaches steady state. Thus, the PMS generates current references as per (22) and PI based current controllers tracks them accurately. *Case (2)* refers to critical Condition E in mode I, which is consequent of Condition B, hence battery and FC current are zero initially. Since, PV power is more than load power and battery has already reached SoC_{BH} hence, SC is charging to maintain the power balance. At instant t_1, SC voltage reaches maximum voltage limit (V_{SCH}). The SC current at instant t_1 is 0.4 A while PV is supplying 1 A and dc link voltage is at reference of 80V. Now, the PV goes into de-rating mode with dc link voltage controller generating the duty ratio (D_3) and subsequently operates PV at off MPPT. The PV current start decreasing at instant t_1, dc link voltage rises slightly above to 82 V and at t_2 the PV current reduces to 0.6 A, Isc reduces to zero and dc link voltage settles to 80 V reference. Thus, power balance is restored. *Case (3)*, system works in Mode II Condition G. Initially at steady state, PV current is 0.2 A while FC supplies 2.5 A, battery supplies 0 A and SC supplies 0.2 A. Now, at instant t_1, load is decreased so FC current decreases slowly to 2 A. At t_2, the battery SoC reaches SoC_{BL}. Hence, I_B reduces to zero while dc link voltage is controlled by SC hence SC current increases to 0.8 A to maintain the power balance, as shown in Fig. 28.

VII. CONCLUSION

The proposed PMS 1 for hybrid AC/DC MG1 successfully drives the MG1 from generation dominating mode to load dominating mode with efficient dc link voltage regulation. The presented PMS is robust to wide variation in operating point. The use of MAF efficiently separates the average current reference to be supplied by fuel cell and battery while transient and oscillatory component of power to be supplied by SC. The proposed MAF based multi-time scale adaptive droop PMS with supervisory control for MG2 offers reliable transition algorithm for operation of multiple PVs and BES in a geographically distributed location. It also considers the SoC charging and discharging rates for multiple BESs. Also, the PMS considers effective utilization of H_2 in FC stack by using current slope limiter. The paper also proposes the control based PV power curtailment under critical conditions. The proposed PMS considers all the contingency conditions. The simulation and experimental results validates the proposed PMS under normal as well as critical conditions. Thus, PV-PEM fuel cell with HES and proposed PMS presents a promising scope for operation as a hybrid AC/DC microgrid.

APPENDIX

Simulation parameters:

PV: V_{mp}=350 V, I_{mp}=28.5 A, P_{mp}=10 KW, L_{pv}=4.5 mH
De-rating loop parameters: Condition B: $K_p = 0.01, K_i = 0.5$ Condition D: $K_p = 0.2, K_i = 2.23$. Droop: R_d=0.2.
PEM FC: R=8314.47, R^{int}=0.00303, $N_0 = 300, E_0 = 0.06$ $F = 96.487 * 10^6$,, $\tau_{h2} = 4.22 * 10^{-5}, \tau_{h20} = 7.71 * 10^{-6}$ $\tau_{02} = 2.11 * 10^{-5}$ $K_{02} = 6.74, K_{H2} = 3.37, K_{H2o} = 18.418,$ $V_{FC} = 348$ V, $P_{FC} = 6$ KW, $L_{FC} = 5\, mH$ $R_{FC} = 0.01\,\Omega$
PI current Control: $K_p = 0.0104$ $K_i = 65.97$. D_{fc}=1/0.2
Battery: $V_B = 350\,V, C_{B1} = 20\,Ahr, L_B = 4.5\,mH, SoC_{BL} = 20\,\%$, $SoC_{BH} = 80\%, K_{pb} = 0.03$ $K_{ib} = 62.3$, C_{B2}=10 Ahr.
SC: $V_{sc} = 375\,V$, $N_{sc} = 160$, $N_p = 1$, $C_{sc} = 10\,F$, $V_{SCL} = 180\,V$, $V_{SCH} = 313.5\,V$, $L_{SC} = 4.5\,mH$, $K_{psc} = 0.025$, $K_{isc} = 36.2$. **DC link:** $V_{dcr} = 700\,V, C_{dc} = 4700\,\mu F, K_{pdc} = 5.29, K_{idc} = 51.72$. D_{sc}=1/0.2. Rc=0.02 ohm.
VSC: $V_o = 380\,V$**,** Rating=25 KVA, L=3mH, C=50 μF, Outer voltage and current loop PI control: $K_{pv} = 0.109$, $K_{iv} = 73.29, K_{pi} = 18.85, K_{ii} = 628.32$.
Experimental parameters: **PV:** $N_s = 4$,$N_p = 3$, $V_{mp} = 72.28$,$P_{mp} = 180\,W$, $L_{pv} = 3\,mH$. Derating loop: Condition B- $K_p = 0.035, K_i = 0.43$ Condition D: $K_p = 0.8, K_i = 5.35$.

This article has been accepted for publication in a future issue of this journal, but has not been fully edited. Content may change prior to final publication. Citation information: DOI 10.1109/TIA.2017.2756032, IEEE Transactions on Industry Applications

PEM FC: 1 KW H-1000 Horizon FC Stack,$V_{FC} = 45\ V$,$N_0 = 48$, $I_{FC} = 40\ A$ (rated), $L_{FC} = 3\ mH$, $K_p = 0.0424$ $K_i = 17.46$. **Lithium-Ion Battery:** $V_B = 48\ V$, $C_B = 20\ Ahr$, $L_B = 3\ mH$, $K_{pb} = 0.62$ $K_{ib} = 23.7$ **SC:** $V_{sc} = 32\ V$, $N_{sc} = 2$, $N_p = 1$,$C_{sc} = 9\ F$,$V_{SCL} = 15\ V$,$V_{SCH} = 28\ V$, $L_{SC} = 3\ mH$, $K_{psc} = 4.69$,$K_{isc} = 43.9$. **Dc link:** $V_{dcr} = 80\ V$, $C_{dc} = 2350\ \mu F$, $K_{pdc} = 12.56$ $K_{idc} = 39.76$ **VSC:** 1 KVA, L=3mH, C=10μF, Vo=50V (L-L) $K_{pv} = 0.087$, $K_{iv} = 14.85$, $K_{pi} = 5.78$, $K_{ii} = 35.78$.

REFERENCES

[1] T. Ma, M. H. Cintuglu and O. A. Mohammed, "Control of a Hybrid AC/DC Microgrid Involving Energy Storage and Pulsed Loads," *IEEE Transactions on Industry Applications*, vol. 53, no. 1, pp. 567-575, Jan.-Feb. 2017.

[2] Xiong Liu, Peng Wang and P. C. Lon, "A hybrid AC/DC microgrid and its coordination control," *IEEE Trans. Smart Grid*, vol. 2, pp. 567-575, June. 2011.

[3] O.C. Onar, M. Uzunoglu and M. S. Alam, "Dynamic modelling, design and simulation of a wind/fuel cell/ultacapacitor based hybrid power generation system," *Journal of Power Sources*, vol. 161, pp. 707-722, Oct. 2006.

[4] M. Y. El-Sharkh *et al*, "A dynamic model for standalone fuel cell power plant for residential applications," *Journal of Power Sources*, vol. 138, pp. 199-204, Nov. 2004.

[5] S. Malo and R. Grino, "Design, Construction, and Control of a Stand-Alone Energy-Conditioning System for PEM-Type Fuel Cells," *IEEE Transactions on Power Electronics*, vol. 25, no. 10, pp. 2496-2506, Oct. 2010.

[6] P. Thounthong, A. Luksanasakul, P. Koseeyaporn and B. Davat, "Intelligent Model-Based Control of a Standalone Photovoltaic/Fuel Cell Power Plant With Supercapacitor Energy Storage," *IEEE Transactions on Sustainable Energy*, vol. 4, no. 1, pp. 240-249, Jan. 2013

[7] S. Sikkabut *et al*., "Control of High-Energy High-Power Densities Storage Devices by Li-ion Battery and Supercapacitor for Fuel Cell/Photovoltaic Hybrid Power Plant for Autonomous System Applications," *IEEE Transactions on Industry Applications*, vol. 52, no. 5, pp. 4395-4407, Sept.-Oct. 2016.

[8] P. Thounthong, S. RaËl and B. Davat, "Control Algorithm of Fuel Cell and Batteries for Distributed Generation System," *IEEE Transactions on Energy Conversion*, vol. 23, no. 1, pp. 148-155, March 2008.

[9] P. Thounthong, S. Rael and B. Davat, "Control Strategy of Fuel Cell and Supercapacitors Association for a Distributed Generation System," *IEEE Transactions on Industrial Electronics*, vol. 54, no. 6, pp. 3225-3233, Dec. 2007.

[10] M. Hamzeh, A. Ghazanfari, H. Mokhtari and H. Karimi, "Integrating Hybrid Power Source Into an Islanded MV Microgrid Using CHB Multilevel Inverter Under Unbalanced and Nonlinear Load Conditions," *IEEE Transactions on Energy Conversion*, vol. 28, no. 3, pp. 643-651, Sept. 2013.

[11] N. R. Tummuru, M. K. Mishra and S. Srinivas, "Dynamic Energy Management of Renewable Grid Integrated Hybrid Energy Storage System," *IEEE Transactions on Industrial Electronics*, vol. 62, no. 12, pp. 7728-7737, Dec. 2015.

[12] N. R. Tummuru, M. K. Mishra and S. Srinivas, "Dynamic Energy Management of Hybrid Energy Storage System With High-Gain PV Converter," *IEEE Transactions on Energy Conversion*, vol. 30, no. 1, pp. 150-160, March 2015.

[13] S. Mishra and R. K. Sharma, "Dynamic power management of PV based islanded microgrid using hybrid energy storage," in *Proc. 2016 IEEE 6th International Conference on Power Systems (ICPS)*, New Delhi, 2016, pp. 1-6.

[14] A. Tani, M. B. Camara and B. Dakyo, "Energy Management in the Decentralized Generation Systems Based on Renewable Energy—Ultracapacitors and Battery to Compensate the Wind/Load Power Fluctuations," *IEEE Transactions on Industry Applications*, vol. 51, no. 2, pp. 1817-1827, March-April 2015.

[15] N. Yang, F. Gao, D. Paire, A. Miraoui and W. Liu, "Distributed control of multi-time scale DC microgrid based on ADRC," *IET Power Electronics*, vol. 10, no. 3, pp. 329-337, 3 10 2017.

[16] Y. Gu, W. Li and X. He, "Frequency-Coordinating Virtual Impedance for Autonomous Power Management of DC Microgrid," *IEEE Transactions on Power Electronics*, vol. 30, no. 4, pp. 2328-2337, April 2015.

[17] Q. Shafiee, T. Dragičević, J. C. Vasquez and J. M. Guerrero, "Hierarchical Control for Multiple DC-Microgrids Clusters," *IEEE Transactions on Energy Conversion*, vol. 29, no. 4, pp. 922-933, Dec. 2014.

[18] Q. Yang; L. Jiang; H. Zhao; H. Zeng, "Autonomous Voltage Regulation and Current Sharing in Islanded Multi-inverter DC Microgrid," *IEEE Transactions on Smart Grid* , vol.PP, no.99, pp.1-1, 2017.

[19] T. Dragičević, J. M. Guerrero, J. C. Vasquez and D. Škrlec, "Supervisory Control of an Adaptive-Droop Regulated DC Microgrid With Battery Management Capability," *IEEE Transactions on Power Electronics*, vol. 29, no. 2, pp. 695-706, Feb. 2014.

[20] Bhattarai, B., Myers, K., Bak-Jensen B., Paudyal S., "Multi-time scale control of demand flexibility in smart distribution networks", *Energies*, *10*, 37, Jan. 2017.

[21] Dinghuan Zhu, "Multi-time scale control of energy storage enabling the integration of variable generation," Ph.D. dissertation, Dept. Of Elect. And Comp. Eng., Carnegie Mellon Univ., PA, 2014.

[22] N. Yang, D. Paire, F. Gao and A. Miraoui, "Distributed control of DC microgrid considering dynamic responses of multiple generation units," in *Proc. IECON 2014 40th Annual Conference of the IEEE Industrial Electronics Society*, Dallas, TX, 2014, pp. 2063-2068.

Rishi Kant Sharma (S'16) received the B.Tech in Electrical Engineering from UPTU, Lucknow, India in 2008 and M.Tech in Control and Instrumentation from Motilal Nehru National Institute of Technology, Allahabad, India in 2010. He has work experience of both academic as well as Industry. He has served as an Assistant Engineer (O&M) in MPPKVVCL, Jabalpur, India. Presently, he is working towards the Ph.D. degree in Electrical Engineering at Indian Institute of Technology Delhi, India.

His research interest lies in the field of advanced controller design, power management and stability analysis of distributed generation in AC/DC microgrid as well as application of hybrid energy storage.

Sukumar Mishra (M'97-SM'04) is a Professor in the Department of Electrical Engineering at the Indian Institute of Technology Delhi. His interest lies in the field of Power Systems, Power Quality Studies, and Renewable Energy. He has published over 100 research articles (including papers in international journals, conferences and book chapters). He is currently holding the position of Vice Chair of Intelligent System Subcommittee of Power and Energy society of IEEE. He is a recipient of the INSA medal for young scientist, the INAE young engineer award, and the INAE silver jubilee young engineer award. He is also a Fellow of IET (UK), NASI (India), INAE (India), IE (India) and IETE (India).

He is working as the NTPC Chair professor and has previously worked as the Power Grid Chair professor. He is also serving as an Independent Director of the Cross Border Power Transmission Company Ltd. and Industry Academic Distinguish Professor. He has handled many research projects and industrial consultancies. He has a vast experience of 25 years and is currently serving as an Editor in IEEE TRANSACTIONS ON SMART GRID and Associate Editor in IET Generation, Transmission & Distribution.